Solid Aluminum Borohydrides for Prospective Hydrogen Storage

Dovgaliuk, Iurii; Safin, Damir; Tumanov, Nikolay; Morelle, Fabrice; Moulai, Adel; Cerný, Radovan; Lodziana, Zbigniew; Devillers, Michel; Filinchuk, Yaroslav

Published in:
ChemSusChem

DOI:
10.1002/cssc.201701629

Publication date:
2017

Document Version
Peer reviewed version

CHEMISTRY & SUSTAINABILITY

CHEMSUSCHEM

ENERGY & MATERIALS

Accepted Article

Title: Solid Aluminum Borohydrides as Perspective Hydrogen Stores

Authors: Iurii Dovgaliuk, Damir Safin, Nikolay Tumanov, Fabrice Morelle, Adel Moulai, Radovan Černý, Zbigniew Łodziana, Michel Devillers, and Yaroslav Filinchuk

To be cited as: *ChemSusChem* 10.1002/cssc.201701629

Link to VoR: http://dx.doi.org/10.1002/cssc.201701629

A Journal of

ChemPubSoc Europe

WILEY-VCH

www.chemsuschem.org

10.1002/cssc.201701629

WILEY-VCH

Solid Aluminum Borohydrides as Perspective Hydrogen Stores

Iurii Dovgaliuk,[a,b] Damir A. Safin,[a] Nikolay A. Tumanov,[a] Fabrice Morelle,[a] Adel Moulai,[a] Radovan Černý,[c] Zbigniew Łodziana,[d] Michel Devillers,[a] and Yaroslav Filinchuk*[a]

Abstract: Metal borohydrides are intensively researched as high capacity hydrogen storage materials. Aluminum is a cheap, light and abundant element and Al^{3+} can be a template for reversible dehydrogenation. However, $Al(BH_4)_3$, containing 16.9 weight % of hydrogen, has a low boiling point, is explosive on air and has poor storage stability. We present a new family of mixed-cation borohydrides $M[Al(BH_4)_4]$, all solid at ambient conditions. Their thermal decomposition properties show diverse behavior: $Al(BH_4)_3$ is released for M = Li^+, Na^+, while heavier derivatives evolve hydrogen and diborane. $NH_4[Al(BH_4)_4]$, containing protic and hydridic hydrogens, has the lowest decomposition temperature of 35 °C and yields $Al(BH_4)_3{\cdot}NHBH$ and hydrogen. The decomposition temperatures, correlated with cations' ionic potential, show that $M[Al(BH_4)_4]$ are in the most practical stability window. This family of solids with convenient and versatile properties puts aluminum borohydride chemistry in the mainstream of the hydrogen storage research, e.g. for the development of reactive hydride composites with increased hydrogen content.

Introduction

Metal borohydrides and their derivatives are of great interest as materials for energy storage due to the high content of hydrogen.[1] Most of alkali and alkali-earth metal borohydrides are matching the recently revised the United States Department of Energy system targets for gravimetric and volumetric hydrogen capacities of 7.5 wt% and 70 g/L, respectively.[2] However, simple metal borohydrides show high stability to pyrolysis, e.g. $LiBH_4$ desorbs hydrogen at ~470 °C, and $Mg(BH_4)_2$ between 290 and 500 °C.[3,4] The decomposition temperature can be tuned and significantly decreased in mixed-metal borohydrides, using the correlation between the decomposition temperature and the Pauling electronegativity of the metal cations.[5–7] The principle standing behind it is the weakening of the B–H bonds in the borohydride with the increase of covalency of the M···H(B) interaction. The destabilization of the latter improves thermal decomposition properties of mixed-metal complex hydrides making some of them suitable for the temperature range of operational fuel cells, 60–120 °C.[8] This includes bimetallic Al-based borohydrides stabilized by chloride substitution,[9,10] as well as Zn- and Cd-based borohydrides stabilized by alkali metals.[11,12]

The favorable decomposition temperatures entail a different problem: metal borohydrides decomposing below 200 °C yield diborane B_2H_6,[13] besides hydrogen, preventing full reversibility of these hydrogen storage systems. One of the known ways to overpass this problem is utilizing reactive hydride composites (RHC): a chemical reaction between two or more hydrides. The reaction products from the mixture of hydrides are different from those released by the individual constituents. Remarkably, the gravimetric hydrogen storage capacity remains as high as the hydrogen storage capacity of the individual hydrides, but the release of the side products, like diborane, can be significantly suppressed. One of the most successful examples of reversible hydrogen storage in the form of complex hydrides is found on addition of MgH_2 to lithium borohydride.[14] The formation of MgB_2 in this system provides destabilization of $LiBH_4$, lowering the hydrogen desorption temperature. There is great interest in finding new H-rich complex hydrides with low decomposition temperatures, especially those with cheap and abundant elements like Al.

Indeed, Al-containing hydrides and composites attract a great deal of attention as hydrogen storage media. In particular, alane AlH_3[15] and alanates of alkali and alkali-earth metals $M(AlH_4)_n$[16] as well as Al-N-B-based hydrides[17] are being intensively investigated. Among the others, $NaAlH_4$ is the most studied alanate due to its high hydrogen content of 5.6 wt% and the Ti-catalyzed reversibility.[18] The following studies demonstrate the reversible hydrogen cycling over 100 cycles with a measured capacity of about 4 wt% at 160 °C.[19] Some Al-based RHCs are also known, i.e. $LiBH_4$–LiH–Al reabsorbs 5.1 wt% of hydrogen at 350 °C under the pressure of 70 bar.[20] The other Al-containing composite, namely $LiBH_4$–MgH_2–Al, reduces the dehydrogenation onset temperature by 100 °C compared to the starting Al-free $LiBH_4$–MgH_2 composite.[21,22] Hence, addition of Al improves some RHCs by lowering their operating temperatures.

Most recently, it was shown that the high polarizing Al^{3+} alters significantly the properties of complex and chemical hydrides, such as borohydrides, ammonia borane etc.[17] Effectively, Al^{3+} is a strong Lewis acid that can serve as a template in chemical transformations of hydrides. Aluminium is capable of coordinating both the initial hydrogenated species as

[a] Dr. Iurii Dovgaliuk, Dr. Damir A. Safin, Dr. Nikolay A. Tumanov, Fabrice Morelle, Mr. Adel Moulai, Prof. Michel Devillers, Prof. Yaroslav Filinchuk
Institute of Condensed Matter and Nanosciences
Université catholique de Louvain
Place L. Pasteur 1, 1348 Louvain-la-Neuve, Belgium
E-mail: yaroslav.filinchuk@uclouvain.be
[b] Dr. Iurii Dovgaliuk
Swiss-Norwegian Beamlines
ESRF - European Synchrotron Radiation Facility
Martyrs, 38042 Grenoble Cedex 9, France
[c] Prof. R. Černý
Laboratory of Crystallography, DQMP
University of Geneva
quai Ernest-Ansermet 24, 1211 Geneva, Switzerland
[d] Prof. Z. Łodziana
Department of Structural Research
INP Polish Academy of Sciences
ul. Radzikowskiego 152, 31-342 Kraków, Poland

Supporting information for this article is given via a link at the end of the document

well as the dehydrogenation products,[23] enabling in some cases a hydrogen desorption reversibility.

Despite of numerous works devoted to the chemistry of boron and aluminum hydrides, neither borohydrides of Al nor their RHCs are well explored so far. This deficiency arises from difficulties of handling the highly pyrophoric and explosive liquid aluminum borohydride, making $Al(BH_4)_3$ highly inconvenient in the experimental work also due to its fast decomposition.[24] Thus, $Al(BH_4)_3$ stabilized in a solid form of $[Al(BH_4)_4]^-$ anions[25] can serve as a platform either for safe $Al(BH_4)_3$ storage, as it was recently proposed by the Ref. [26], or for a design of novel RHCs. This beneficial feature can be used not only for hydrogen storage, but also in the technological processes, such as fabrication of the light-emitting wide gap $Al_{1-x}B_x$ semiconductor technology (e.g.$Al_{1-x}B_xPSi_3$)[27] as well as a perspective green bipropellant rocket fuel.[28]

In this work, we report on the synthesis, crystal structures, thermal analysis, Raman and NMR spectroscopy studies together with the detailed DFT calculations of a series of $Al(BH_4)_3$-based mixed-cation borohydrides, $M[Al(BH_4)_4]$ ($M = Li^+$, Na^+, K^+, NH_4^+, Rb^+, Cs^+). We show that the members of the series decompose between 35 and 150 °C yielding a variety of products, including $Al(BH_4)_3$, H_2 and B_2H_6. The stability of the new series is related to the ionic potential of metal atoms and is favorable compared to other known metal borohydrides. The thermodynamic assessment of the RHCs using $M[Al(BH_4)_4]$ with light metal hydrides suggests potentially reversible hydrogen storage in these systems.

Results and Discussion

All mixed-cation borohydrides were obtained by the addition reaction of $Al(BH_4)_3$ and MBH_4 ($M = Li^+$, Na^+, K^+, NH_4^+, Rb^+, Cs^+). $NH_4[Al(BH_4)_4]$ was produced with an almost qualitative yield of 97.3(9) wt%, while the alkali metal borohydrides had to be ground and soaked in $Al(BH_4)_3$ from two to four times to reach high yields. The fact that several milling/soaking cycles are required can be explained by the formation of $M[Al(BH_4)_4]$ on the surface of MBH_4, hence preventing the completion of the reaction. Below we briefly describe the interaction of $Al(BH_4)_3$ with MBH_4, products of their decomposition, crystal structures of the obtained phases and evaluate the stability of the Al-based borohydride series with respect to other known borohydrides.

Formation and thermal stability of the mixed-cation aluminum borohydrides. The synchrotron X-ray powder diffraction reveals the whole series of the mixed-cation $M[Al(BH_4)_4]$ ($M = Li^+$, Na^+, K^+, NH_4^+, Rb^+, Cs^+). The diffraction data were used to solve the new crystal structures (see below) and the variable temperature diffraction studies allowed to characterize their thermal decomposition, see Fig. 1 and Figs. S1-S3 in the supporting information. The reaction with $LiBH_4$ produces two different mixed-metal complexes, $Li[Al(BH_4)_4]$ and $Li_4Al_3(BH_4)_{13}$, shown on Fig. 1. $Li[Al(BH_4)_4]$ was not known so far, while $Li_4Al_3(BH_4)_{13}$ is found to be isostructural to the Cl-substituted $Li_4Al_3(BH_4)_{12.74}Cl_{0.26}$ obtained by ball milling $AlCl_3$ with $LiBH_4$.[9] $Li_4Al_3(BH_4)_{13}$ is more stable at room temperature as the diffraction peaks of $Li[Al(BH_4)_4]$ gradually decrease on heating and completely vanish at about 60 °C, see Fig. 1. The amount of $Li_4Al_3(BH_4)_{13}$ abruptly increases at the same temperature, thus the following reaction can be stated:

$$4Li[Al(BH_4)_4] \rightarrow Li_4Al_3(BH_4)_{13} + Al(BH_4)_3 \quad (1)$$

Note that the boiling point of $Al(BH_4)_3$ is 44 °C and thus it can not be observed by diffraction. The complementary measurements using TGA and DSC in the range of 50–90 °C exhibit one endothermic decomposition step with the maximum at 89 °C (Fig. S4, top). Thus, $Li_4Al_3(BH_4)_{13}$ is a major phase at 60–80 °C but it completely decomposes already at about 90 °C, releasing $Al(BH_4)_3$ and $LiBH_4$ according to the known reaction:[25b]

$$Li_4Al_3(BH_4)_{13} \rightarrow 4LiBH_4 + 3Al(BH_4)_3 \quad (2)$$

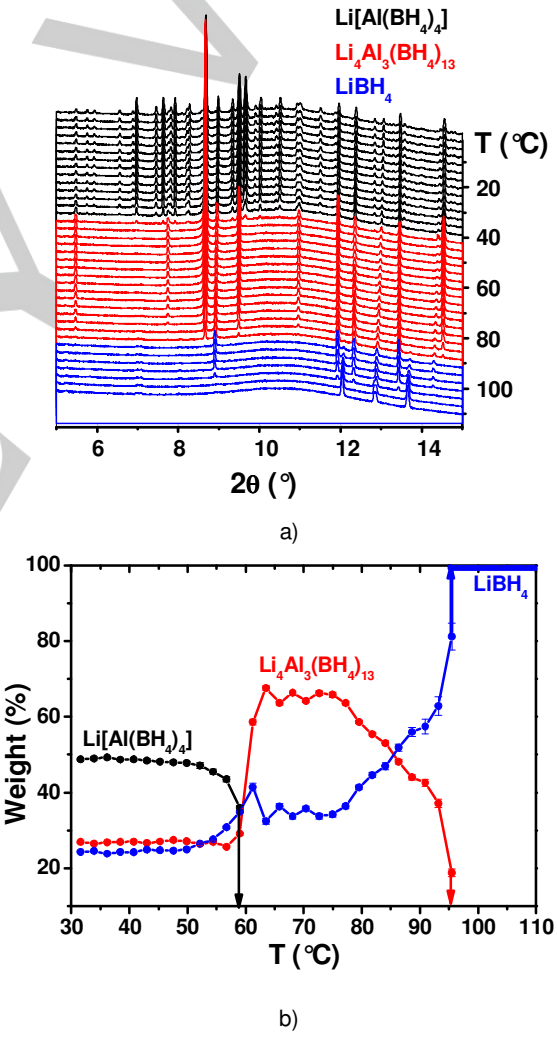

Figure 1. a) The variable temperature in-situ plot of the powder patterns of $Li[Al(BH_4)_4]$, $Li_4Al_3(BH_4)_{13}$ and $LiBH_4$. b) The mass fractions extracted from the Rietveld refinement on in-situ XRPD patterns (Materials Science Beamline, PSI, Mythen II detector, λ = 0.775045 Å).

In-situ diffraction shows that the heavier $M[Al(BH_4)_4]$ decompose at slightly higher temperatures: at 90 °C for M = Na (Fig. S1), at 160 °C for M = K [26, 29] and Rb (Fig. S2), and at ~150 °C for M = Cs (Fig. S3). According to TGA and DSC (Fig. S4), $Na[Al(BH_4)_4]$ decomposes at 70–110 °C, the mass loss corresponds to the extraction of the volatile aluminum borohydride. Considering the formation of $NaBH_4$ seen by the XRPD, the following equation can be stated:

$$Na[Al(BH_4)_4] \rightarrow NaBH_4 + Al(BH_4)_3 \quad (3)$$

Contrary to the light $M[Al(BH_4)_4]$ (M = Li^+, Na^+, K^+), forming the corresponding crystalline MBH_4, the intensities of $RbBH_4$ and $CsBH_4$ raise insignificantly upon the decomposition of the Al-based hydride. The increased background upon the thermal decomposition of the HT-$Cs[Al(BH_4)_4]$ at ~150 °C indicates the formation of the amorphous product(s), while some amount of the cubic $CsBH_4$ forms only upon further heating above 165 °C. The TGA plots for $Rb[Al(BH_4)_4]$ and $Cs[Al(BH_4)_4]$ contain two poorly defined decomposition steps with the total weight loss of 13.2 and 4.5%, respectively (Fig. S5). These values are significantly lower than 41.6 and 32.6 wt% expected for the release of the volatile $Al(BH_4)_3$. Nevertheless, the weight loss for $Rb[Al(BH_4)_4]$ is higher than the calculated hydrogen content of 9.4 wt%, suggesting a release of heavier gases. Indeed, according to the TGA-MS and volumetric data, the first decomposition step of $Rb[Al(BH_4)_4]$ is accompanied by the release of hydrogen and diborane, while only hydrogen is detected during the second decomposition step (giving 4 moles of gas, in total, per mole of $Rb[Al(BH_4)_4]$, see Figs. S6 and S7). On the contrary, the total weight loss by $Cs[Al(BH_4)_4]$ of 4.5% is smaller than the calculated hydrogen content of ~7.4 wt% (4.5 mol of gas in total, see Fig. S7). This might be an indication for the release of pure hydrogen upon the thermal decomposition. However, the TGA-MS and volumetric data show the simultaneous release of hydrogen and diborane during the first decomposition step (Figs. S7 and S8 in the Supporting Information), and the release of hydrogen only during the second step, similar to the behavior of the Rb-containing analogue. Interestingly, the previous theoretical investigations of $Rb[Al(BH_4)_4]$ and $Cs[Al(BH_4)_4]$ clusters suggested their higher stability with respect to fragmentation into MBH_4 and $Al(BH_4)_3$, compared to $K[Al(BH_4)_4]$.[26] This is in agreement with the present periodic calculations (Figure 3), however our experimental observations can be explained by a formation of the decomposition products different from MBH_4 and $Al(BH_4)_3$.

$NH_4[Al(BH_4)_4]$ will be discussed separately due to its unique thermal decomposition behavior. It arises from the coexistence of the protic H^+ and hydridic H^- hydrogens forming dihydrogen bonds in the structure, which easily recombine even on slight heating. The XRPD reveals the formation of nearly pure $NH_4[Al(BH_4)_4]$ (Fig. S9 in the Supporting Information). This compound is the most unstable within the series and melts with a decomposition at 35 °C. It does not form the initial NH_4BH_4 upon the decomposition, but a number of species related to the dehydrogenation of the mixed-cation borohydride as a whole.

TGA data on the sample containing ~97 wt% of the crystalline $NH_4[Al(BH_4)_4]$ reveal two clearly defined decomposition steps (Fig. S10). The decomposition of the complex starts at about 35 °C with the weight loss of ~13.6%, while the second decomposition step occurs at 58 °C and reveals ~20.5% weight loss. The similar two step weigh loss was also observed upon the thermal decomposition of $Al(BH_4)_3{\cdot}NH_3BH_3$.[23] According to the TGA-MS data on $NH_4[Al(BH_4)_4]$, both decomposition steps are accompanied by the release of hydrogen, diborane and ammonia (Fig. S11). No detectable amounts of $Al(BH_4)_3$ were observed by mass spectrometry. Complementary volumetric studies, performed at the constant temperature of 40 °C, reveals the release of about 3 moles of gas per more of $NH_4[Al(BH_4)_4]$ (Fig. S12) during the first decomposition step.

To clarify the nature of the decomposition products of $NH_4[Al(BH_4)_4]$, ^{11}B, $^{11}B\{^1H\}$, ^{27}Al, $^{27}Al\{^1H\}$ and ^1H NMR spectroscopy experiments were performed in toluene-d_8. The freshly dissolved sample was studied, as well as the toluene solutions aged at room temperature for 2 and 10 days. The attribution of signals is given in the supporting information. The main decomposition product is $Al(BH_4)_3{\cdot}NHBH$, previously identified as the main product of $Al(BH_4)_3{\cdot}NH_3BH_3$ dehydrogenation.[23] In addition, there is a secondary reaction pathway leading to $Al(BH_4)_3$, slowly decomposing to $[HAl(BH_4)_2]$ and B_2H_6. The MS measurements on the gases evolving from the solid $NH_4[Al(BH_4)_4]$ (Fig. S10) show no $Al(BH_4)_3$, and, hence, this reaction path is characteristic for the solution in toluene-d_8. The main decomposition pathway both in toluene (as seen by NMR) and in solvent-free conditions (as seen by the volumetric and DSC/TGA-MS methods) can be described by the following reaction:

$$NH_4[Al(BH_4)_4] \rightarrow Al(BH_4)_3{\cdot}NHBH + 3H_2 \quad (4)$$

Notably, neither NMR spectroscopy in solution nor the in-situ XRPD on the crystalline $NH_4[Al(BH_4)_4]$ detect the formation of $Al(BH_4)_3{\cdot}NH_3BH_3$,[23] expected as an intermediate by analogy with the perovskite type $NH_4Ca(BH_4)_3$, transforming into $Ca(BH_4)_2{\cdot}NH_3BH_3$.[30,31]

To summarize on the formation and stability of the Al-based borohydrides, we conclude that the Li–Al and Na–Al borohydrides can be seen as convenient stores of aluminum borohydride, as they are stable at room temperature with no significant amount of polymerization to higher boranes typical for $Al(BH_4)_3$.[32] The latter can be obtained upon heating the bimetallic compounds to moderate temperatures (60–90 °C). The heavier $M[Al(BH_4)_4]$ (M = K^+, Rb^+, Cs^+) irreversibly release hydrogen (no readsorption even at $p(H_2)$ = 100 bar) and some improvements should be implemented for their practical applications. In particular, we surmise the possibility of making the RHCs, as discussed below.

Crystal Structures of the mixed-cation aluminum borohydrides. All the crystal structures were determined from synchrotron powder diffraction data, and post-optimized by the DFT methods, see the experimental section and the supporting information for details. $Li[Al(BH_4)_4]$ crystallizes in the monoclinic space group $P2_1/c$ with four independent cations and complex anions. All the Li^+ and Al^{3+} cations are surrounded by four BH_4^- anions, coordinated *via* edges (Fig. 2). As a result of these interactions, a 3D framework constructed from distorted $[Al(BH_4)_4]^-$ "supertetrahedra" is formed, resembling the structure

of $LiBH_4$.[33] The underlying net, as analyzed by the program TOPOS,[34] is a 4-connected net of a new type containing four nods (two Li^+ and two Al^{3+}) with the point symbol $\{4.6^2.8^3\}\{4.6^4.8\}$. The framework character of the compound is underlined by a similar distance between Li^+ and Al^{3+} from bridging BH_4^- when normalized to the sum of the ionic radii (cation + anion), see the supporting information for more details of the molecular geometry in the crystal structures.

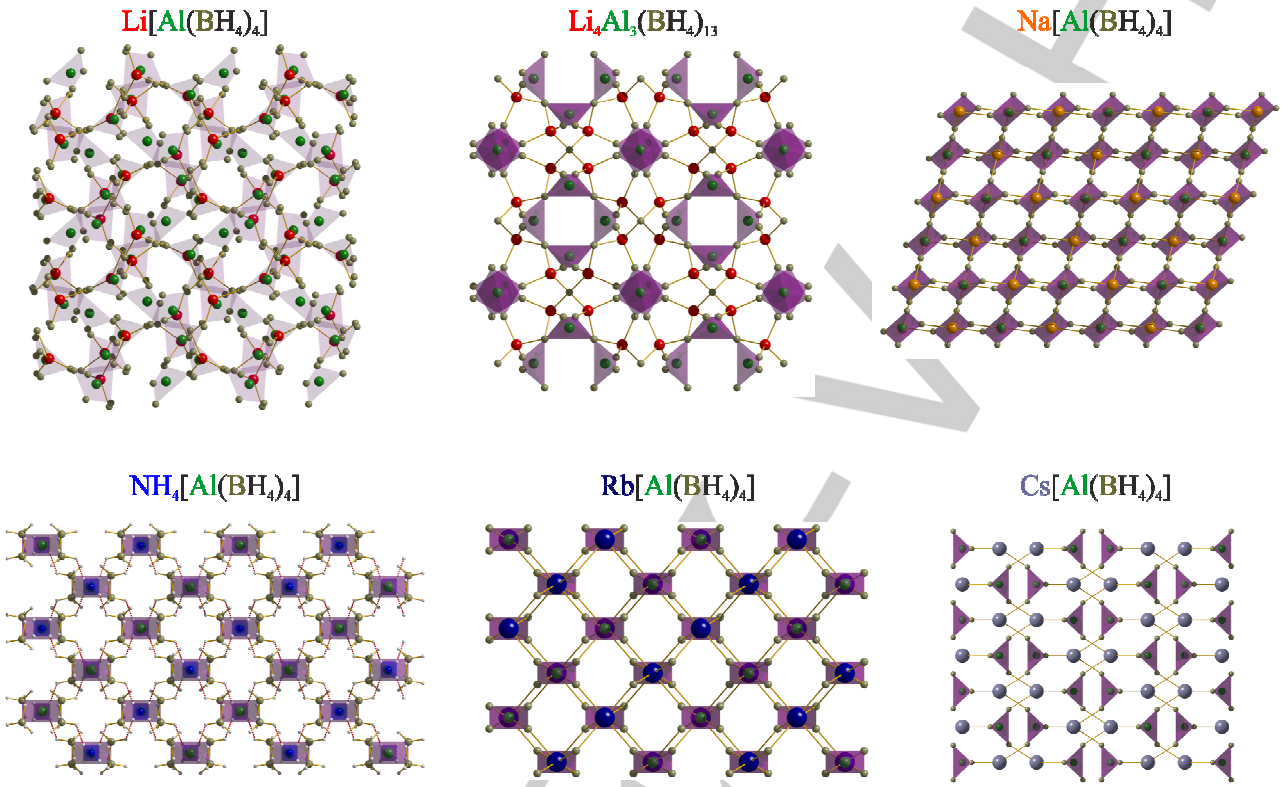

Figure 2. Crystal packing of the mixed-cation aluminum borohydride frameworks along the *a* ($Li[Al(BH_4)_4]$) and *b* axes. The complex $[Al(BH_4)_4]^-$ anions are represented as flattened purple "supertetrahedra", where hydrogens are omitted for clarity (except the ones in $NH_4[Al(BH_4)_4]$, which contains red dihydrogen bonds between BH_4^- and NH_4^+ ions). Color code: Al – green, B – olive, H – grey, Li – red, Na – orange, N – blue, Rb – blue dark, Cs – blue grey.

$Li_4Al_3(BH_4)_{13}$ crystallizes in the cubic *P*–43*n* space group, with a structure identical to the previously published $Li_4Al_3(BH_4)_{12.74}Cl_{0.26}$.[8] The composition of these compounds can be rationalized on the basis of a complex cation $[(BH_4)Li_4]^{3+}$ and an anion $[Al(BH_4)_4]^-$, packed like in the Frank-Kasper Cr_3Si-type phase.[8] We want to point out that our topology analysis indicates that $[(BH_4)Li_4][Al(BH_4)_4]_3$ is an antitype of Ag_3PO_4.[35]

$Na[Al(BH_4)_4]$ crystallizes in the monoclinic space group *C*2/*c*. The Na^+ atom is in a distorted octahedral coordination environment formed by six BH_4^- groups coordinated *via* edges (Fig. 2). This coordination is typical in other Na-containing borohydrides, *e.g.* $Na[Al(BH_4)_{4-x}Cl_x]$[10] and $NaBH_4$.[36] Importantly, $Na[Al(BH_4)_4]$ takes a different structure, with 90° reorientation of the complex anion with respect to the Na^+ countercations, than in the Cl-substituted phase.[10] Its structure is a monoclinic deformation of $Na[Sc(BH_4)_4]$,[37] which itself is of the $CrVO_4$-type. Each $[Na(BH_4)_6]^{5+}$ octahedron in the structure of $Na[Al(BH_4)_4]$ is linked *via* edges to the neighboring octahedra, producing layers, which in turn are linked by vertices to the tetrahedral $[Al(BH_4)_4]^-$ anions (Fig. 2).

The crystal structure of $K[Al(BH_4)_4]$ was reported earlier in the space group *Fddd*[29] and in its subgroup *Fdd*2.[26] We have made the normal mode analysis for the *Fdd2* structure and found that the structure is stable with respect to atomic displacements. However, the simulated annealing procedure applied to this phase resulted in the stable *Fddd* symmetry (Table S1 in the Supporting Information). The ground state electronic energy and the zero point energy of the structure with the *Fddd* symmetry equals within 1 meV/f.u. with those for the *Fdd2* one. Therefore, we can confirm the higher space group symmetry *Fddd* for $K[Al(BH_4)_4]$.[29] In this work we found that $NH_4[Al(BH_4)_4]$ and $Rb[Al(BH_4)_4]$ are isomorphous to the K-containing analogue with the *Fddd* structure.[29] An important difference for the former case is the presence of the short dihydrogen $(N)H^{\sigma+}\cdots H^{\sigma-}(B)$ bonds (Fig. 2). The experimental H···H distance of 1.82 Å is confirmed by the DFT calculations (Table S1 in the Supporting Information), and found to be significantly shorter than those in NH_3BH_3 (1.91(5) Å)[38] and in NH_4BH_4 (2.28 Å).[39]

The high temperature polymorph of $Cs[Al(BH_4)_4]$ crystallizes in the tetragonal space group $I4_1/amd$. Its crystal structure is derived from the scheelite-type,[40] which is also the prototype of another mixed-cation borohydride $Cs[Y(BH_4)_4]$.[41] The powder pattern of the room temperature polymorph was indexed in a monoclinic unit cell which points towards a structural relation known between scheelite and monazite.[42] In spite of the significant efforts, no reliable structural model was obtained for the room temperature polymorph. In the HT polymorph, the Cs^+ cation coordinates (4 + 8) BH_4^- groups with the Cs···B distances of 3.66(7) and 4.53(3) Å (Fig. 2). The adjacent coordination polyhedra are sharing pseudo square faces (4.01 × 4.43 $Å^2$), resulting in the formation of an infinite 3D framework.

Raman Spectroscopy. The Raman spectra of $M[Al(BH_4)_4]$ (M = Li^+, Na^+, NH_4^+, Rb^+, Cs^+) each contain bands for the B–H bending and stretching modes of the BH_4^- ligands in the $[Al(BH_4)_4]^-$ anion at 1000–1500 cm^{-1} and 2100–2600 cm^{-1}, respectively (Figure S14 in the Supporting Information). The stretching mode bands are characteristic for the bidentately coordinated borohydride anions.[43] The same was observed in the Raman spectrum of $K[Al(BH_4)_4]$.[29] The complex anion $[Al(BH_4)_4]^-$ is also visible in the Raman spectra due to the presence of the characteristic band at about 460 cm^{-1}, arising from the Al···H–B stretching mode. Besides all, the Raman spectrum of $Na[Al(BH_4)_4]$ contains a characteristic band for $NaBH_4$, centered at about 2330 cm^{-1}. The spectrum of $Li[Al(BH_4)_4]$ is further complicated by the presence of bands for $LiBH_4$ and $Li_4Al_3(BH_4)_{13}$.

Formation energies. In order to delineate the thermodynamic parameters of the $M[Al(BH_4)_4]$ series for potential application in RHCs, the enthalpy of formation for the $M[Al(BH_4)_4]$ series and for $Li_4Al_3(BH_4)_{13}$ was calculated from the ground state energies of the corresponding structures and of the starting $Al(BH_4)_3$ and MBH_4 (Fig. 3). The *Pna*2 structure was used for $Al(BH_4)_3$ as a reference.[44] The low temperature structures were used for MBH_4 as described recently.[45] The $P4_2/nmc$ symmetry was applied for the MBH_4 (M = Rb^+, Cs^+) structures, whereas according to our calculations the lowest energy structure of NH_4BH_4 has the $P\text{–}42_1c$ symmetry. However, the latter structure is unstable with respect to the orientation of NH_4^+ (imaginary modes related to the NH_4^+ rotation) as well as to the decomposition into NH_3BH_3 and H_2.[46] Therefore, two sets of data, corresponding to the decomposition into disordered/unstable NH_4BH_4 and to the decomposition into NH_3BH_3 and H_2, are shown for $NH_4[Al(BH_4)_4]$ (Fig. 3). The error bar accounts for four imaginary modes related to the NH_4^+ librations. The calculated enthalpies indicate that all compounds are stable with respect to the decomposition into binary borohydrides, and this stability increases for heavier alkali metals. There is an additional decomposition path for $Li[Al(BH_4)_4]$ according to the equation 1 with experimentally observed $Li_4Al_3(BH_4)_{13}$. The calculated electronic contribution to the enthalpy of this reaction is –0.29 eV/f.u. The zero point vibrations increase this enthalpy up to –0.15 eV/f.u.

The reaction $NH_3BH_3 + H_2 \rightarrow NH_4BH_4$ is endothermic with calculated ΔH = +0.15 ÷ 0.42 eV/f.u., that is reflected in the lower stability of $NH_4[Al(BH_4)_4]$ compared to $NH_3BH_3 + H_2$ (Fig. 3).

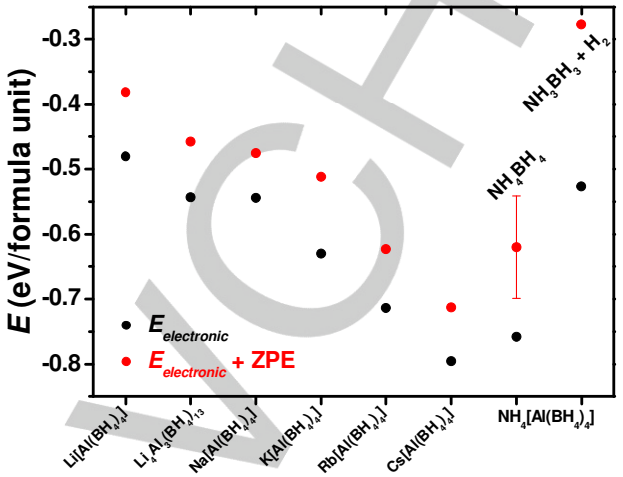

Figure 3. Calculated enthalpies of formation of mixed-cation borohydrides from one mole of $Al(BH_4)_3$ and the corresponding MBH_4. Black circles are for the ground state electronic energy and red circles account for the zero point vibrations.

Composition-structure-stability relations. The first attempt to explain the stability of the Al-based series of borohydrides is based on the first Pauling's rule,[47] stating in particular that the cation-anion radius ratio (r_C/r_A) determines the coordination number of the cation.

The Li^+ cation in $Li[Al(BH_4)_4]$ adopts a tetrahedral coordination environment by the BH_4^- groups, matching the stability window defined by the r_C/r_A ratio (Fig. 4). Nevertheless, this compound exhibits relatively low thermal stability. The Na^+ cation in $Na[Al(BH_4)_4]$ has an octahedral environment by the BH_4^- groups, as expected for the given r_C/r_A ratio (Fig. 4), and is more stable than its Li-based analogue. The K^+-, Rb^+- and Cs^+-containing derivatives have similar and relatively high stability (Fig. 4). Their coordination numbers range from 4+4 to 4+8, being higher than the typical value of 6 in this r_C/r_A window. The $[(BH_4)Li_4]^{3+}$ is significantly larger than the other cations and falls into the stability region of the icosahedral coordination, considering the much larger $[Al(BH_4)_4]^-$ anion. Indeed, this cation has the expected icosahedral coordination by the complex anions (Fig. 4), but the stability of $[(BH_4)Li_4][Al(BH_4)_4]_3$ is much lower than for M = K^+, Rb^+ and Cs^+. The radius of the $[Al(BH_4)_4]^-$ anion was found, based on the crystal structure data of the described borohydrides, to be equal ~3 Å. $NH_4[Al(BH_4)_4]$ is in a special position, as it has the same structure and the r_C/r_A ratio as for M = K^+, Rb^+, but it is much less stable, likely due to the formation of the $(N)H^{\sigma+}\cdots H^{\sigma-}(B)$ dihydrogen bonds (Fig. 2), which easily recombine into H_2.

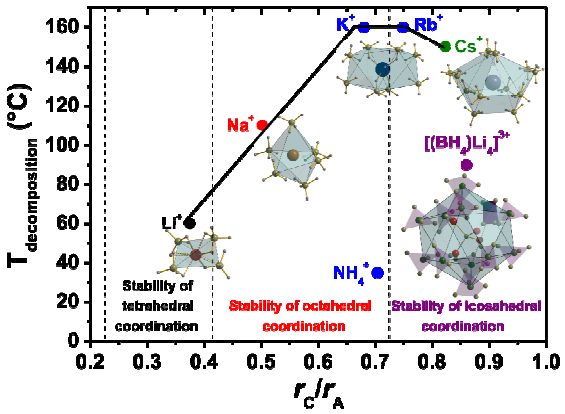

Figure 4. Thermal stability of $M[Al(BH_4)_4]$ (M = Li^+, Na^+, K^+, NH_4^+, Rb^+, Cs^+) and of $[(BH_4)Li_4][Al(BH_4)_4]_3$ as a function of the cation-anion ratio. The dashed lines define the stability regions of the coordination polyhedra according to the first Pauling's rule. The observed coordination environments (colored circles: black – tetrahedral, red – octahedral, blue – 4+4, olive – 4+8, purple – icosahedral, the latter is based on the size ratio for the complex cation and the complex anion) do not fully match the stability regions. The observed mismatch does not explain the variation of the decomposition temperatures.

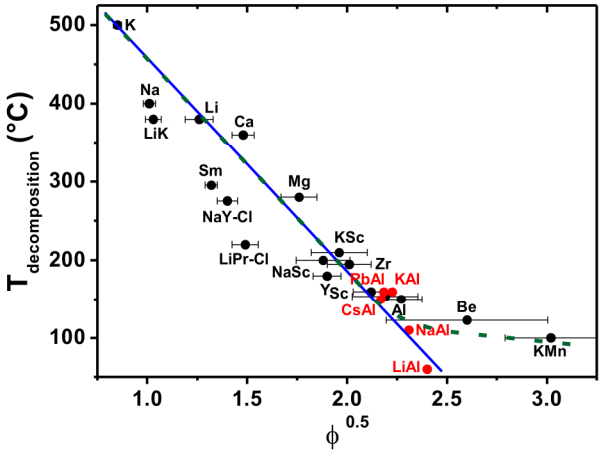

Figure 5. The experimental decomposition temperatures of metal borohydrides as a function of the ionic potential obtained using the calculated dynamical charges on cations. The results of the present work are shown as red circles, while the data shown as black circles were taken from Ref. [45]. Highly polarized metal cations shift the linearity of the fitted curve (dashed green).

We can thus conclude that the observed coordination numbers do not match well the stability regions deduced from the geometrical principles of the first Pauling's rule. Moreover, the observed mismatches do not explain the variation of the decomposition temperatures. Therefore, in the second attempt to address the structure-property relation, we had to take into account the electronic factors.

The relation between the formation enthalpy of metal borohydrides (Fig. 5) and the Pauling electronegativity,[5–7] has driven the idea of synthesis of mixed-cation borohydrides aiming to tune the decomposition temperature. This semi-empirical rule holds well for alkali metals, however deviation is observed for the compounds containing transition metals or metals with a higher oxidation state. Recently, it was shown that the ionic potential ($\varphi = Z^*/r$, where r is the ionic radius of a cation) provides a simple measure of the stability of mixed-cation borohydrides,[45] as long as the Born effective charges are taken as the charge of cations. The Born effective charges measure polarization induced by the displacement of ions, thus they are sensitive to the nature of interatomic bonding within the crystal and to the site symmetry of ions.

We have calculated the Born effective charges for the members of the title series and matched them with the decomposition temperatures (Fig. 5). The decomposition temperatures of the new compounds reported in this work are depicted in red, and those for the common metal borohydrides are in black. The data follow the linear regression of the decomposition temperature vs. the ionic potential. All the Al-based borohydrides are located in the region of high ionic potentials with $\varphi^{0.5}$ higher than 2.

The Al-based bimetallic compounds combining even stronger polarizing Mg^{2+} or Ca^{2+} cations, would lead to the decomposition at room temperature, and thus are most likely unstable under ambient conditions. Indeed, our attempts to isolate bimetallic borohydrides in the $Mg(BH_4)_2$–$Al(BH_4)_3$ and $Ca(BH_4)_2$–$Al(BH_4)_3$ systems were unsuccessful. Consequently, the title family of Al-based borohydrides is complete in practical terms: any new members with higher ionic potential will be too unstable for applications. Nevertheless, the diverse family presented here, having convenient and versatile decomposition properties, puts aluminum borohydrides into the mainstream research in hydrogen storage, e.g. for the development of reactive hydride composites with an increased hydrogen content

Thermodynamic evaluation of mixed cation aluminum borohydrides in RHCs. The optimal stability, versatility of the decomposition reaction pathways, the low cost of raw materials and the exceptional hydrogen storage densities make these compounds highly interesting for the design of new reactive hydride composites involving metal hydrides, such as MgH_2 or CaH_2.[48] The thermodynamic evaluation was done using the calculated formation enthalpies for the Al-based series from the corresponding monometallic borohydrides (Fig. 3), omitting the formation entropy term, the formation energy of LiAl at 415 °C[49] and the thermodynamic data for MgB_2 from Ref. [50]. The thermodynamics of possible decomposition pathways indicates that all the reactions are endothermic, and can be potentially reversible by applying hydrogen pressure:

$$Li[Al(BH_4)_4] + 2\ MgH_2 \rightarrow 2\ MgB_2 + LiAl + 10\ H_2 \quad (5)$$
$$\Delta H^0 = 13.5\ kJ/mol\ H_2,\ \Delta S^0 = 84.1\ J/K{\cdot}mol\ H_2$$
$$[(BH_4)Li_4][Al(BH_4)_4]_3 + 6.5\ MgH_2 \rightarrow 6.5\ MgB_2 + 3\ LiAl + LiH + 32H_2 \quad (6)$$
$$\Delta H^0 = 16.0\ kJ/mol\ H_2,\ \Delta S^0 = 84.6\ J/K{\cdot}mol\ H_2$$
$$Na[Al(BH_4)_4] + 2\ MgH_2 \rightarrow 2\ MgB_2 + NaH + Al + 9.5\ H_2 \quad (7)$$
$$\Delta H^0 = 14.0\ kJ/mol\ H_2,\ \Delta S^0 = 88.3\ J/K{\cdot}mol\ H_2$$

The estimated hydrogen pressure required for the rehydrogenation at 295 °C is 100 bar for the reaction (5), 39 bar for the reaction (6) and 136 bar for the reaction (7).

The synthesis of $M[Al(BH_4)_4]$ precursors can be scaled up using mechanochemical methods, making the synthesis also much cheaper. Remarkably, ball milling of $AlCl_3$ with MBH_4 yields the light members of the series[9,10] with still high hydrogen capacity in the resulting mixtures, e.g. 7.7 wt% for $[(BH_4)Li_4][Al(BH_4)_4]_3$ + LiCl, compared to 17.2 wt % for the pure $[(BH_4)Li_4][Al(BH_4)_4]_3$). The thermodynamically feasible reactions 6 and 7 between the ball-milled $[(BH_4)Li_4][Al(BH_4)_4]_3$ + LiCl or $Na[Al(BH_4)_{4-x}Cl_x]$ + NaCl with MgH_2 do not occur neither at room temperature nor upon heating. The thermal decomposition of $[(BH_4)Li_4][Al(BH_4)_4]_3$ and $Na[Al(BH_4)_{4-x}Cl_x]$ starts at lower temperatures than the reactions 6 and 7, see Figs. S15 and S16. The use of hydrogen back-pressure may change this behaviour to more favourable, thus more attempts should be made, using also more reactive alkali metal hydrides.

Conclusions

A new family of Al-based hydrogen-rich borohydrides $M[Al(BH_4)_4]$ ($M = Li^+$, Na^+, K^+, NH_4^+, Rb^+, Cs^+) was obtained by the reaction of solid MBH_4 with liquid $Al(BH_4)_3$. The thermal decomposition properties of $M[Al(BH_4)_4]$ are diverse: $Al(BH_4)_3$ is released below 100 °C for $M = Li^+$ and Na^+, while heavier derivatives evolve hydrogen and diborane at about 150 °C. $NH_4[Al(BH_4)_4]$ occupies a special place, as it contains protic and hydridic hydrogens, recombining into hydrogen already at 35 °C. Its major decomposition product is $Al(BH_4)_3{\cdot}NHBH$, recently observed upon thermal decomposition of $Al(BH_4)_3{\cdot}NH_3BH_3$.[23] $M[Al(BH_4)_4]$ can be seen as a convenient store of the highly unstable aluminum borohydride, as well as extremely H-rich substances suitable for the design of new hydrogen (energy) storage materials. With its diversity, convenient and versatile decomposition properties, the aluminum borohydrides shall be put into the mainstream research in hydrogen storage, e.g. for the development of reactive hydride composites with an increased hydrogen content.

Experimental Section

Materials: All reactions were performed using commercially available reagents: $AlCl_3$, $LiBH_4$, $NaBH_4$ (from Sigma Aldrich with >95 % purity), $LiBH_4$ (from Boss chemical industry Co., China with 96 % purity), $RbBH_4$, $CsBH_4$ (from Katchem), NH_4F (from Sigma Aldrich with 98.8 % purity) and anhydrous NH_3 (from Praxair).

Raman Spectroscopy: Spectra were recorded at room temperature with a Bruker RFS 100/s FT-Raman spectrometer (I = 200 mW) in the 100–4000 cm^{-1} range, using a diode-pumped, air-cooled Nd:YAG laser with 1064 nm excitation.

NMR Spectroscopy: NMR spectra in toluene-d_8 were collected on a Bruker Avance DRX500 spectrometer operating at 500.13 for ^1H, 160.461 MHz for ^{11}B and 130.318 MHz for ^{27}Al nuclei. Chemical shifts are reported with reference to $SiMe_4$ (TMS) for ^1H, $BF_3{\cdot}OEt_2$ for ^{11}B and 1.1 M of $Al(NO_3)_3$ in D_2O for ^{27}Al.

Thermal Analysis: Thermogravimetric analysis (TGA) and differential scanning calorimetry (DSC) were performed on powder samples. TGA of $M[Al(BH_4)_4]$ ($M = Li^+$, Na^+) were performed using a PerkinElmer STA 6000 apparatus. The samples (~2 mg) were loaded into an Al_2O_3 crucible and heated from room temperature to 400 °C (5 °C/min heating rate) in a dynamic argon flow of 20 mL/min. $NH_4[Al(BH_4)_4]$ was measured on a TGA/DTA 851 Mettler instrument (1 °C/min heating rate) from 25 to 150 °C with a dynamic nitrogen flow of 100 mL/min. All the samples for thermal analysis were loaded in the argon-filled glove box.

Volumetric Analysis and Reversibility Tests: Volumetric analysis was performed using a Hiden Isochema IMI-SHP analyzer. $NH_4[Al(BH_4)_4]$ (~40 mg) was heated from 30 to 40 °C (1 °C/min, p(He) = 1 bar) and kept at this temperature for ~2 weeks. $M[Al(BH_4)_4]$ ($M = Rb^+$, Cs^+) were heated from 30 to 160 °C (5 °C/min, p(He) = 1 bar). Subsequently, the gas release for all experiments was calculated from the calibrated volumes of the system, excluding the volume of the glass wool (2.06 g/cm^3 density) and samples' skeletal volumes taken from their crystal structures. The rehydrogenation of remaining solid residues were performed, applying $p(H_2)$ = 100 bar at 40 °C for $NH_4[Al(BH_4)_4]$ and 160 °C for $M[Al(BH_4)_4]$ ($M = Rb^+$, Cs^+), respectively.

Synthesis of $Al(BH_4)_3$: Caution! $Al(BH_4)_3$, which was synthesized as recently described,[29] is highly pyrophoric liquid which explodes on contact with air. All manipulations were carried out in a dedicated nitrogen-filled Plexiglas dry box.

Synthesis of Ammonium Borohydride (NH_4BH_4): Ammonium borohydride was synthesized by a slightly modified procedure[51] *via* a metathesis reaction between ammonium fluoride and sodium borohydride in liquid ammonia: $NaBH_4 + NH_4F \rightarrow NH_4BH_4 + NaF$. Stoichiometric amounts of ammonium fluoride and sodium borohydride were weighted in the argon-filled glove box and loaded together with a magnetic stirrer into a round bottom flask №1 equipped with a glass filter. The flask was connected to a Schlenk line and kept under slight argon overpressure to avoid moisture contamination. Ammonia gas was first condensed at –78 °C, using a coldfinger condenser filled with dry ice and acetone, in a Schlenk flask №2, containing a small amount of sodium metal, to ensure complete dryness. When the desired amount of liquefied ammonia (100 mL) was obtained, the ammonia bottle was disconnected and the condenser was replaced on flask №1, thus dry ammonia evaporated from flask №2 and was recondensed into flask №1. Once the ammonia transfer was complete, the reaction was left while stirring at reflux for 1 h. Then the solution was filtrated to remove precipitated sodium fluoride and the solvent was removed in vacuum. The resulting product was transferred in the argon-filled glove box and kept in the freezer at –35 °C. Due to the high instability of ammonium borohydride one of the main challenges of this synthetic procedure is to keep the product at low temperature during synthesis and transfer from the Schlenk line to the storage freezer.

Synthesis of $M[Al(BH_4)_4]$ ($M = Li^+$, Na^+, K^+, NH_4^+, Rb^+, Cs^+): $K[Al(BH_4)_4]$ was prepared according to the recently described procedure.[29] Other mixed-cation borohydrides were obtained similar to the potassium-containing analogue, according to the following reaction: $Al(BH_4)_3 + MBH_4 \rightarrow M[Al(BH_4)_4]$. Freshly prepared $Al(BH_4)_3$ (1–4 mL) was transferred *via* a syringe into the flask, containing ground powders of MBH_4 (100–200 mg, $M = Li^+$, Na^+, NH_4^+, Rb^+, Cs^+) and stirred for 4–7 days. The reaction with NH_4BH_4 was done at –35 °C in the glovebox freezer. The excess of volatile $Al(BH_4)_3$ was removed in vacuum. According to the X-ray powder diffraction (XRPD), the yield of

$NH_4[Al(BH_4)_4]$ is 97.3(9) wt% already after the first soaking cycle, owing to the high reactivity of ammonium borohydrides and partly thanks to the low temperature preventing the decomposition of the final product. However, for MBH_4 ($M = Na^+$, Rb^+, Cs^+), the first cycle of soaking in $Al(BH_4)_3$ yielded mixtures of $M[Al(BH_4)_4]$ and MBH_4 in about 1:1 weight ratio. The yield of the targeted products was significantly increased, up to ~90 wt%, after the second soaking of the well-ground mixtures of $M[Al(BH_4)_4]/MBH_4$ in $Al(BH_4)_3$. The formation of $Li[Al(BH_4)_4]$ is always accompanied by $Li_4Al_3(BH_4)_{13}$ and four cycles were required to obtain ~85 wt% yield. Light $M[Al(BH_4)_4]$ ($M = Li^+$, Na^+, NH_4^+) are unstable at room temperature and should be stored in the fridge (typically at –35 °C). Attention must be paid when washing the glassware after synthesis of light $M[Al(BH_4)_4]$ ($M = Li^+$, Na^+, NH_4^+), as the traces of their powders react vigorously with water. The alcohol should be used first.

Mechanochemical preparation of $Li_4Al_3(BH_4)_{12.74}Cl_{0.26}$, $Na[Al(BH_4)_{4-x}Cl_x]$ and their MgH_2 reactive hydrides composites. The chlorine-containing analogues of $[(BH_4)Li_4][Al(BH_4)_4]_3$ and $Na[Al(BH_4)_4]$ have been prepared by the previously described mechanochemical procedures.[9,10] The formation of $Li_4Al_3(BH_4)_{12.74}Cl_{0.26}$ and $Na[Al(BH_4)_{4-x}Cl_x]$ was confirmed by the laboratory X-ray powder diffraction. For the preparation of composites, the same procedure was used with addition of MgH_2 to the starting mixtures with the following proportions: $3AlCl_3 + 13LiBH_4 + 6.5MgH_2$ and $AlCl_3 + 4NaBH_4 + 6.5\ MgH_2$. The obtained composites contained the mixtures of $Li_4Al_3(BH_4)_{12.74}Cl_{0.26}$ + LiCl or $Na[Al(BH_4)_{4-x}Cl_x]$ + NaCl with MgH_2.

Variable Temperature In-situ Synchrotron X-ray Powder Diffraction and Crystal Structure Determination: Samples were filled under high purity argon atmosphere into 0.5 and 0.7 mm thin-walled glass capillaries. Laboratory diffraction data were obtained with MAR345 diffractometer equipped with a rotating anode (MoKα radiation) and a XENOCS focusing mirror.

The crystal structure of $Li[Al(BH_4)_4]$ was solved from data collected at varied temperatures at the Materials Science Beamline at PSI (Villigen, Switzerland), using Mythen II detector and λ = 0.775045 Å. The temperature was increased linearly in time with 5 °C/min heating rate. The unit cell was indexed using FOX,[52] and the space group $P2_1/c$ was found by ChekCell.[53] In order to ease the structure solution, the anion $[Al(BH_4)_4]^-$ was modeled as a rigid body, using the structural data of $K[Al(BH_4)_4]$. For that, the anion with 21 atom was transformed from the special position in the original *Fddd* space group to the general position in the *P*1 subgroup using PowderCell.[54] The obtained coordinates were transformed into a *z*-matrix with the program OpenBabel.[55] Finally, four independent $[Al(BH_4)_4]^-$ anions were transferred into FOX and optimized with Li^+ cations. The resulting structure was refined by Rietveld method in Fullprof (Figure S15 in the Supporting Information),[56] and later validated by DFT calculations (see below).

The crystal structure of $Li_4Al_3(BH_4)_{13}$ was refined using the model of the previously known structure of $Li_4Al_3(BH_4)_{12.74}Cl_{0.26}$, which contained some chloride atoms on the borohydride sites[56] (Figure S18 in the Supporting Information).

The crystal structure of $Na[Al(BH_4)_4]$ was solved from *in-situ* synchrotron XRPD data collected at SNBL/ESRF (Grenoble, France) with PILATUS 2M pixel detector and λ = 0.823065 Å. The temperature was increased linearly in time at 5 °C/min rate. The unit cell was indexed and the structure was solved in the space group *Cc* using FOX.[52] The final refinement was performed from the synchrotron XRPD data, collected on Materials Science Beamline at PSI (Villigen, Switzerland), using Mythen II detector and λ = 0.775045 Å. ADDSYM routine in the program PLATON[57] suggested the *C*2/*c* space group. The resulting Rietveld refinement profile was obtained from the DFT optimized structure, where boron and hydrogen atomic positions as well as atomic displacement parameters were refined by full matrix in Fullprof (Figure S19 in the Supporting Information).[56]

The crystal structures of $NH_4[Al(BH_4)_4]$ and $Rb[Al(BH_4)_4]$ each were solved from *in-situ* synchrotron XRPD data collected at SNBL/ESRF (Grenoble, France) with PILATUS 2M pixel detector and λ = 0.68884 and 0.682525 Å, respectively. Temperature was increased linearly in time using Oxford Cryostream 700+ at a 5 °C/min heating rate. The 2D images were azimuthally integrated with Bubble software that performs azimuthal integration of raw images.[58] The unit cells were indexed in the *Fddd* space group by DICVOL.[59] The structures were found to be isomorphous to $K[Al(BH_4)_4]$[23] and refined by Rietveld method in Fullprof (Figure S20 and S21 in the Supporting Information)[56] with the NH_4^+ and BH_4^- groups as semi-rigid tetrahedra with common refined B–H and N–H distances of 1.20 and 1.04 Å, respectively. No other restraints were used.

The crystal structure of $Cs[Al(BH_4)_4]$ was solved from variable temperature *in-situ* XRPD data collected at the Materials Science Beamline at PSI (Villigen, Switzerland), using Mythen II detector and λ = 0.775045 Å. The temperature was increased linearly in time with 5 °C/min rate. The unit cell was indexed in the $I4_1/amd$ space group by DICVOL,[59] and the structure was solved in FOX[52] and refined by the Rietveld method using Fullprof (Figure S22 in the Supporting Information).[56]

DFT Calculations: The structure analysis was performed for all compounds in order to check and confirm thermodynamic stability and refine positions of the hydrogen atoms. The calculations were performed within periodic plane wave expansion of the electronic wave functions and Density Functional Theory (DFT) formalism as implemented in VASP package.[60] The electronic configuration of elements was represented by projected augmented wave[61] potentials with the following valence states: $1s^1$ for H, $1s^22s^1$ for Li, $2s^22p^1$ for B, $2s^22p^3$ for N, $2p^63s^1$ for Na, $3p^64s^1$ for K, $4s^24p^65s^1$ for Rb and $5s^25p^66s^1$ for Cs. The gradient corrected (GGA) exchange correlation functional was used.[62]

Static structural optimization was performed with a conjugate gradient method; for each structure the internal atomic positions as well as the lattice parameters were optimized until forces exerted on atoms were smaller than 0.01 eV/Å. The experimentally determined configurations were used as starting ones, and the crystal symmetry was constrained during initial structure optimization. Afterwards a simulated annealing search for the possible more stable configuration was performed. This was done by heating the structure to 350 K at the rate of 100 K/ps and cooling it down to 0 K at the rate of 50 K/ps. No constraints were imposed on the internal atomic positions and the unit cell parameters were kept fixed during the annealing process. Nosé-Hoover thermostat[63] was applied for this procedure, and the time step for integration of equations of motion was 0.6 fs. The symmetry of each system was analyzed[64] after the simulated annealing procedure. Any new symmetry was re-optimized with methods used for the static calculations. For all structures the normal modes were analyzed. The normal mode frequencies were calculated at the Γ point by displacing the symmetry non-equivalent atoms in each crystallographic direction by ±0.01 Å.

In order to compare thermodynamic stability of the mixed-cation compounds at the ground state with respect to the decomposition into $Al(BH_4)_3$ and corresponding MBH_4 ($M = Li^+$, Na^+, K^+, NH_4^+, Rb^+, Cs^+), the structural optimization and normal mode analysis were performed for all the relevant phases. The energy cutoff was increased to 600 eV for the calculations of the ground state energy. The enthalpy of the reaction was calculated as $\Delta H = E(M[Al(BH_4)_4]) - E(Al(BH_4)_3) - E(MBH_4) +$

$E_0(M[Al(BH_4)_4]) - E_0(Al(BH_4)_3) - E_0(MBH_4)$, where E is the ground state energy and E_0 is the contribution from zero point vibrations ($E_0 = \sum h\omega_i/2$).

The Born effective charges Z^*[65] were calculated for $M[Al(BH_4)_4]$ (M = Li^+, Na^+, K^+, Rb^+, Cs^+) (**Tables S2** and **S3** in the Supporting Information). The isotropic component of Z^* is equal to one-third of the trace. The ionic radii for cations are based on the Shannon data.[66]

Acknowledgements

This work was supported by the Académie Universitaire Louvain (AUL, Belgium) under Grant ADi/DB/1058.2011 and FNRS (CC 1.5169.12, PDR T.0169.13, EQP U.N038.13). R. Černý acknowledges the support from the Swiss National Science Foundation. We thank ESRF and PSI for the beam time allocation at SNBL and MS beamline at SLS respectively. The research leading to these results has received funding from the European Community's Seventh Framework Programme (FP7/2007-2013) under grant agreement n. 312284 (CALIPSO). Z. Łodziana acknowledges CPU time allocation at PLGrid Infrastructure and the support by a grant from Switzerland through the Swiss Contribution to the enlarged European Union.

Keywords: high-energy materials • hydrogen storage • stability • crystal structure

[1] a) M. Paskevicius, L. H. Jepsen, P. Schouwink, R. Černý, D. B. Ravnsbæk, Y. Filinchuk, M. Dornheim, F. Besenbacher, T. R. Jensen, *Chem. Soc. Rev.* **2017**, *46*, 1565–1634; b) R. Mohtadi, A. Remhof, P. Jena, *J. Phys. Cond. Mat.* **2016**, *28*, 353001.

[2] L. E. Klebanoff, J. O. Keller, *Int. J. Hydrogen Energy*, **2013**, *38*, 4533–4576.

[3] A. Züttel, S. Rentsch, P. Fischerb, P. Wengera, P. Sudana, Ph. Maurona, Ch. Emmenegger, *J. Alloys Compd.* **2003**, 356–357, 515–520.

[4] K. Chłopek, C. Frommen, A. Lèon, O. Zabara, M. Fichtner, *J. Mater. Chem.* **2007**, *17*, 3496–3503.

[5] G. N. Schrauzer, Naturwissenschaften 1955, 42, 438.

[6] Y. Nakamori, K. Miwa, A. Ninomiya, H. Li, N. Ohba, S. Towata, A. Züttel, S. Orimo, *Phys. Rev. B* **2006**, *74*, 45126.

[7] L. H. Rude, T. K. Nielsen, D. B. Ravnsbæk, U. Bösenberg, M. B. Ley, B. Richter, L. M. Arnbjerg, M. Dornheim, Y. Filinchuk, F. Besenbacher, T. R. Jensen, *Phys. Status Solidi A* **2011**, *208*, 1754–1773.

[8] W. Grochala, P. P. Edwards, *Chem. Rev.* **2004**, *104*, 1283–1315.

[9] I. Lindemann, R. D. Ferrer, L. Dunsch, Y. Filinchuk, R. Černý, H. Hagemann, V. D'Anna, L. M. L. Daku, L. Schultz, O. Gutfleisch, *Chem. Eur. J.* **2010**, *16*, 8707–8712.

[10] I. Lindemann, R. D. Ferrer, L. Dunsch, R. Černý, H. Hagemann, V. D'Anna, Y. Filinchuk, L. Schultz, O. Gutfleisch, *Faraday Discuss.* **2011**, *151*, 231–242.

[11] D. B. Ravnsbæk, Y. Filinchuk, Y. Cerenius, H. J. Jakobsen, F. Besenbacher, J. Skibsted, T. R. Jensen, *Angew. Chem. Int. Ed.* **2009**, *48*, 6659–6663.

[12] D. Ravnsbæk, L. H. Sørensen, Y. Filinchuk, F. Besenbacher, T. R. Jensen, *Angew. Chem. Int. Ed.* **2012**, *51*, 3582–3586.

[13] O. Friedrichs, A. Remhof, A. Borgschulte, F. Buchter, S. I. Orimo, A. Züttel, *Phys. Chem. Chem. Phys.* **2010**, *12*, 10919–10922.

[14] J. J. Vajo, S. L. Skeith, *J. Phys. Chem. B* **2005**, *109*, 3719–3722.

[15] J. Graetz, J. J. Reilly, V. A. Yartys, J. P. Maehlen, B. M. Bulychev, V. E. Antonov, B. P. Tarasov, I. E. Gabis, *J. Alloys Compd.* **2011**, *509*, S517–S528.

[16] J. Graetz, B. C. Hauback, *MRS Bulletin* **2013**, *38*, 473–479.

[17] I. Dovgaliuk, Y. Filinchuk *Int. J. Hydrogen Energy* **2016**, *41*, 15489–15504.

[18] B. Bogdanovich, M. Schwickardi, *J. Alloys Compd.* **1997**, *254–256*, 1–9.

[19] S. S. Srinivasan, H. W. Brinks, B. C. Hauback, D. Sun, C. M. Jensen, *J. Alloys Compd.* **2004**, *377*, 283–289.

[20] S.-A. Jin, J.-H. Shim, Y. W. Cho, K.-W. Yi, O. Zabara, M. Fichtner, *Scripta Materialia* **2008**, *58*, 963–965.

[21] Y. Zhang, Q. Tian, H. Chu, J. Zhang, L. Sun, J. Sun, Z. Wen, *J. Phys. Chem. C* **2009**, *113*, 21964–21969.

[22] B. R. S. Hansen, D. B. Ravnsbæk, J. Skibsted, T. R. Jensen, *Phys. Chem. Chem. Phys.* **2014**, *16*, 8970–8980.

[23] I. Dovgaliuk, C. Le Duff, K. Robeyns, M. Devillers, Y. Filinchuk, *Chem. Mater.* **2015**, *27*, 768–777.

[24] H. I. Schlesinger, R. T. Sanderson, A. B. Burg, *J. Am. Chem. Soc.* **1940**, *62*, 3421–3425.

[25] a) K. N. Semenenko, O. V. Kravchenko, *Russ. J. Neorg. Chem.* **1972**, *17*, 1084–1086; b) I. Lindemann, A. Borgschulte, E. Callini, A. Züttel, L. Schultz, O. Gutfleisch, *Int. J. Hydrogen Energy* **2013**, *38*, 2790–2795.

[26] D. A. Knight, R. Zidan, R. Lascola, R. Mohtadi, C. Ling, P. Sivasubramanian, J. A. Kaduk, S.-J. Hwang, D. Samanta, P. Jena, *J. Phys. Chem. C* **2013**, *117*, 19905–19915.

[27] P. Sims, T. Aoki, R. Favaro, P. Wallace, A. White, C. Xu, J. Menendez, J. Kouvetakis, *Chem. Mater.* **2015**, *27*, 3030–3039.

[28] S. Schneider, T. Hawkins, Y. Ahmed, M. R. L. Hudgens, J. Mills *Angew. Chem. Int. Ed.* **2011**, *50*, 5886–5888.

[29] I. Dovgaliuk, V. Ban, Y. Sadikin, R. Černý, L. Aranda, N. Casati, M. Devillers, Y. Filinchuk, *J. Phys. Chem. C* **2014**, *118*, 145–153.

[30] P. Schounwink, B. M. Ley, A. Tissot, H. Hagemann, T. R. Jensen, L. Smrčok, R. Černý, *Nature Commun.* **2014**, *5*, 5706.

[31] P. Schouwink, F. Morelle, Y. Sadikin, Y. Filinchuk, R. Černý, *Energies* **2015**, *8*, 8286–8299.

[32] A. J. Downs, L. A. Jones, *Polyhedron* **1994**, *13*, 2401–2415.

[33] J.-Ph. Soulié, G. Renaudin, R. Černý, K. Yvon, *J. Alloys Compd.* **2002**, *346*, 200–205.

[34] V. A. Blatov, *Struct. Chem.* **2012**, *23*, 955–963.

[35] a) J. M. Newsam, A. K. Cheetham, B. C. Tofield, *Solid State Ionics* **1980**, *1*, 377–393; b) R.W.G. Wyckoff, *Z. Kristallogr.* **1925**, *62*, 529–539

[36] Y. Filinchuk, D. Chernyshov, V. Dmitriev, *Z. Kristallogr.* **2008**, *223*, 649–659.

[37] R. Černý, G. Severa, D. B. Ravnsbæk, Y. Filinchuk, V. D'Anna, H. Hagemann, D. Haase, G. M. Jensen, T. R. Jensen, *J. Phys. Chem. C* **2010**, *114*, 1357–1364.

[38] M. E. Bowden, G. J. Gainsford, W. T. Robinson, *Aust. J. Chem.* **2007**, *60*, 149–153.

[39] R. Flacau, C. I. Ratcliffe, S. Desgreniers, Y. Yao, D. D. Klug, P. Pallister, I. L. Moudrakovski, J. A. Ripmeester, *Chem. Commun.* **2010**, *46*, 9164–9166.

[40] L. G. Sillén, A. L. Nylander, *Ark. Kemi Mineral. Geol.* **1943**, *17A*, 1–27.

[41] T. Jaroń, W. Wegner, W. Grochala, *Dalton Trans.* **2013**, *42*, 6886–6893.

[42] M. P. Kokkoros, *Prakt. Athener Akad.* **1942**, *17*, 163–174.

[43] T. J. Marks, J. R. Kolb,*Chem. Rev.* **1977**, *77*, 263–293.

[44] S. Aldridge, A. J. Blake, A. J. Downs, R. O. Gould, S. Parsons, C. R. Pulham, *J. Chem. Soc., Dalton Trans.* **1997**, 1007–1012.

[45] P. Błoński, Z. Łodziana, *Phys. Rev. B* **2014**, *90*, 054114.

[46] M. Gutowski, T. Autrey, *Prepr. Pap.-Am. Chem. Soc., Div. Fuel Chem.* **2004**, *49*, 275–276.

[47] L. Pauling, *J. Am. Chem. Soc.* **1929**, *51*, 1010–1026.

[48] L. H. Jepsen, M. B. Ley, Y. Su-Lee, Y. W. Cho, M. Dornheim, J. O. Jensen, Y. Filinchuk, J. E. Jørgensen, F. Besenbacher, T. R. Jensen, *Mater. Today* **2014**, *17*, 129–135.

[49] C. J. Wen, B. A. Boukamp, R. A. Huggin, *J. Electrochem. Soc.* **1979**, 126, 2258–2266.
[50] G. Balducci, S. Brutti, A. Ciccioli, G. Gigli, P. Manfrinetti, A. Palenzona, M.F. Butman, L. Kudin, *J. Phys. Chem. Sol.*, **2005**, *66*, 292–297.
[51] R. W. Parry, D. R. Schultz, P. R. Girardot, *J. Am. Chem. Soc.*,**1958**, *80*, 1–3.
[52] V. Favre-Nicolin, R. Černý, *J. Appl. Crystallogr.*, **2002**, *35*, 734–743.
[53] LMGP-Suite Suite of Programs for the interpretation of X-ray Experiments, by Jean laugier and Bernard Bochu, ENSP/Laboratoire des Matériaux et du Génie Physique, BP 46. 38042 Saint Martin d'Hères, France. WWW: http://www.inpg.fr/LMGP and http://www.ccp14.ac.uk/tutorial/lmgp/.
[54] W. Kraus, G. Nolze, *J. Appl. Crystallogr.* **1996**, *29*, 301–303.
[55] N. M. O'Boyle, M. Banck, C. A. James, C. Morley, T. Vandermeersch, G. R. Hutchison, *J. Cheminformatics* **2011**, *3*, 33.
[56] J. Rodriguez-Carvajal, *J. Physica B*. **1993**, *192*, 55–69.
[57] A. L. Spek, PLATON. University of Utrecht, The Netherlands, **2006**.
[58] V. Dyadkin, P. Pattison, V. Dmitriev, D. Chernyshov, *J. Synchrotron Rad.* **2016**, *23*, 825–829.
[59] J. Rodriguez-Carvajal, *J. Physica B*. **1993**, *192*, 55–69.
[60] G. Kresse, J. Furthmüller, *Phys Rev B* **1996**, *54*, 11169.
[61] P. E. Blöchl, *Phys. Rev. B* **1994**, *50*, 17953.
[62] J. P. Perdew, K. Burke, M. Ernzerhof, *Phys. Rev. Lett.* **1996**, *77*, 3865.
[63] S. Nosé, *J. Chem. Phys.* **1984**, *81*, 511–519.
[64] H. T. Stokes, D. M. Hatch, *J. Appl. Cryst.* **2005**, *38*, 237–238.
[65] M. Born and K. Huang, *Dynamical Theory of Crystal Lattices*, Oxford University Press, Oxford, UK, **1954**.
[66] R. D. Shannon, *Acta Crystallogr.* **1976**, *A32*, 751–767.

10.1002/cssc.201701629

WILEY-VCH

Entry for the Table of Contents

FULL PAPER

Aluminum is a cheap, light and abundant element and Al^{3+} can be a template for reversible dehydrogenation. A new family of $M[Al(BH_4)_4]$, all solid at ambient conditions, show diverse thermal decomposition properties and the optimal stability window. They are promising for development of reactive hydride composites with increased hydrogen content.

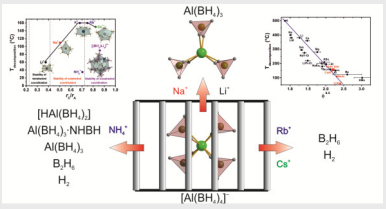

*Iurii Dovgaliuk, Damir A. Safin, Nikolay A. Tumanov, Fabrice Morelle, Adel Moulai, Radovan Černý, Zbigniew Łodziana, Michel Devillers, Yaroslav Filinchuk**

Page No. – Page No.

Solid Aluminum Borohydrides as Perspective Hydrogen Stores